Destabilization of Solitons through Quantum Fluctuations

Mbuso Khanyani MATFUNJWA (mbuso@aims.ac.za)
African Institute for Mathematical Sciences (AIMS)

Supervised by: Prof. Herbert Weigel
Stellenbosch University, South Africa

23 May 2019

Submitted in partial fulfillment of a structured masters degree at AIMS South Africa

Abstract

We study the ϕ^8 scalar field model and compute the kinks (topological solutions) of this model in (1+1) dimensions. We also study quantum fluctuations around these soliton solutions. In doing so we must solve a scattering problem. Phase shifts of the solitons are computed from a scattering matrix we obtain from the scattering problem. We also study the Born approximation and vacuum polarization energies (VPE), which are corrections to the classical energy. VPE have bound and scattering contributions. The latter are obtained from the density of states, which are related to the phase shifts that we compute in this work. The ϕ^8 scalar field model has different masses at positive and negative spatial infinity for some model parameters. In this case the VPE may destabilise the soliton.

Declaration

I, the undersigned, hereby declare that the work contained in this research project is my original work, and that any work done by others or by myself previously has been acknowledged and referenced accordingly.

Mbuso Khanyani Matfunjwa, 23 May 2019

Contents

Abstract i

1 Introduction 1
1.1 Soliton . . . 1

2 The ϕ^8 field theory 4
2.1 Kinks in (1+1) dimensions . . . 4
2.2 Kink Fluctuations . . . 5
2.3 Phase shifts . . . 6
2.4 Bound States . . . 7
2.5 Vacuum Polarization Energy . . . 9

3 Numerical results 12
3.1 Kinks of the ϕ^8 model . . . 12
3.2 Phase Shifts and Born approximation . . . 19

4 Conclusion 22
4.1 Future work . . . 22

References 25

1. Introduction

There are several different models that have soliton solutions. One can think of solitons as solutions to some fundamental classical field equation (Manton and Sutcliffe, 2004), with localized energy density. We will further discuss solitons in Section 1.1. In theoretical physics there is growing interest in non-linear soliton models, especially topological solitons in (1+1) dimensions. This interest is noticeable in a wide range of fields in theoretical physics, from condensed matter to cosmology (Vilenkin and Shellard, 2000) and high energy physics. It is motivated by the fact that (1+1) dimensional models are used to describe various physical systems (Belendryasova and Gani, 2019). Various phenomena emerge from systems of these models, including escape windows in multi-soliton collisions with non-radiative exchange of energy and kink resonant interactions with barriers and wells (Marjaneh et al., 2017).

A kink is a stable travelling wave solution that either descends or rises from one asymptotic state to another. It has all its derivatives going to zero rapidly outside a localized region. Kink dynamics can be studied using different methods. These methods include quasi-exact methods like numerical solutions to partial differential equations derived from equations of motion. Other methods include collective coordinate approximation (Gani et al., 2014) and Manton's method (Marjaneh et al., 2017). The ϕ^8 model solutions have been computed by Gani et al. (2015), but we will numerically calculate them again. We devote Chapter 2 to the ϕ^8 field theory and a description of its properties. We will discuss kinks and kink fluctuations. We also briefly discuss phase shifts and bound states which are the essential ingredients for the vacuum polarization energies (VPE).

An essential feature of the ϕ^8 soliton is that it produces different curvatures for the fluctuations at negative and positive spatial infinity, i.e., different mass parameters. In turn this may lead to an unbounded VPE that destabilizes the soliton. This property has been observed for other solitons (Weigel, 2017; Weigel and Graham, 2018) and is the main motivation for the present investigation. We present our main results in Chapter 3. The results we present will include the kink solutions and the phase shifts. These are essential in the computation of the density of states $\rho(k)$. The change in the density of states $\Delta\rho(k)$ will be an important quantity when we compute the VPEs. We also show some details of the calculations we carried out. In Chapter 4 we conclude and look at future prospects.

1.1 Soliton

A soliton is a solitary wave that possesses specific properties. A solitary wave is a stable and localized solution to a non-linear equation that is not dispersive. A solitary wave can also be defined as a translational wave that is a result of the balance between dispersive and non-linear effects. Some of the properties of a soliton include (Drazin and Johnson, 1989):

i) permanent form (or shape),

ii) localization within a region,

iii) keeps shape after an interaction (or collision) with other solitons, only shifted in phase.

The first known observation of solitary waves was made by John Scott Russell, a scientist and engineer from Scotland in 1834 (MacPherson, 1989). He observed a solitary wave in a canal and he reproduced his observation in his home in a tank. His work seemed odd at the time since it could not be explained by the available wave theories. It was in the 1870s when a theoretical explanation and solution was published

by Joseph Boussinesq and Lord Rayleigh. Then in 1895, the Korteweg-de Vries (KdV) equation was introduced by Diederik Korteweg and Gustav de Vries. They included in their publication the conoidal wave and solitary wave solutions (Korteweg and De Vries, 1895). Zabusky and Kruskal (1965) produced a computational demonstration of soliton-like behavior with KdV in 1965.

An inverse scattering transform was discovered by Gardner, Greene, Kruskal and Miura in 1967. This is very important when solving the KdV equation analytically. In recent years solitons have been studied in a wide variety of fields. They have many different applications in biology (Scott, 1992), particle physics, fibre optics (Yousefi and Muminov, 2012) and magnetics (Kosevich et al., 1998), to mention but a few. Solitons can be classified into topological and non-topological solitons (Yousefi and Muminov, 2012), although there are other ways of classifying them. The simplest examples of topological solitons are kinks on the real line. Other examples occur in field theory models in two or more spatial dimensions. These include magnetic monopoles in three dimensions, vortices in two dimensions (both being gauge theory solitons), and Skyrmions (Skyrme, 1961).

There are a variety of field theories in (1+1) dimensions. These include the ϕ^4 model, which has been well studied. This model only has two equilibria (in its potential), but some physical systems have more equilibria. This makes way for what we call higher order field theories. These include ϕ^6, ϕ^8 models and beyond (Saxena et al., 2019). In this essay we will concentrate on the ϕ^8 model, but we will quickly introduce the ϕ^6 model below.

1.1.1 ϕ^6 model. We define the model by the following Lagrangian,

$$\mathcal{L} = \frac{1}{2}\partial_\mu\phi\partial^\mu\phi - V(\phi). \tag{1.1.1}$$

In Equation (1.1.1), V(ϕ) is the potential which defines the self-interactions of the scalar field, ϕ, and takes the form,

$$V(\phi) = \frac{1}{2}\phi^2(1-\phi^2)^2. \tag{1.1.2}$$

The Lagrangian (together with the potential) gives the field equation

$$\frac{\partial^2\phi}{\partial t^2} - \frac{\partial^2\phi}{\partial x^2} = -3\phi^5 + 4\phi^3 - \phi. \tag{1.1.3}$$

Since we will only consider static solutions, we must solve

$$\frac{\partial^2\phi}{\partial x^2} = 3\phi^5 - 4\phi^3 + \phi, \tag{1.1.4}$$

with solutions of the form

$$\phi(x) = \pm\sqrt{\frac{1}{2}(1 \pm \tanh(x))}. \tag{1.1.5}$$

We have shown a plot of the potential in Figure 1.1(a). The potential has three vacua (degenerate minima) at $\phi = 0, \pm 1$, so there are two kinks interpolating between these vacua. It is worth noting that the potential has different curvatures at these minima. The kinks are shown in Figures 1.1(b) and 1.1(c), together with their corresponding antikinks.

1.1.2 Notation. In our calculations we will denote

$$\mu = (0, 1) = (t, x),$$

and the metric

$$g_{\mu\nu} = \begin{pmatrix} 1 & 0 \\ 0 & -1 \end{pmatrix},$$

will be useful when dealing with the Lagrangian. For simplicity, we set $m = c = \hbar = 1$.

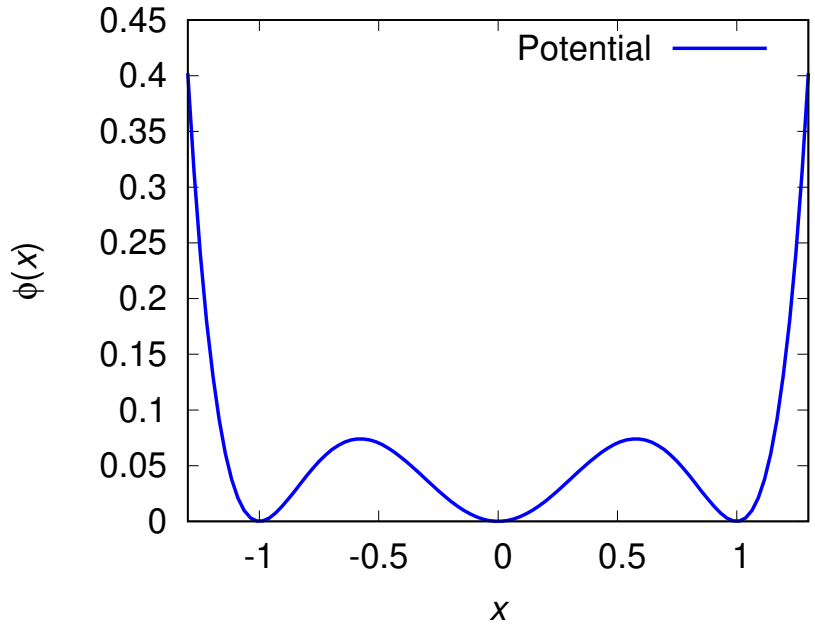

(a) ϕ^6 model potential.

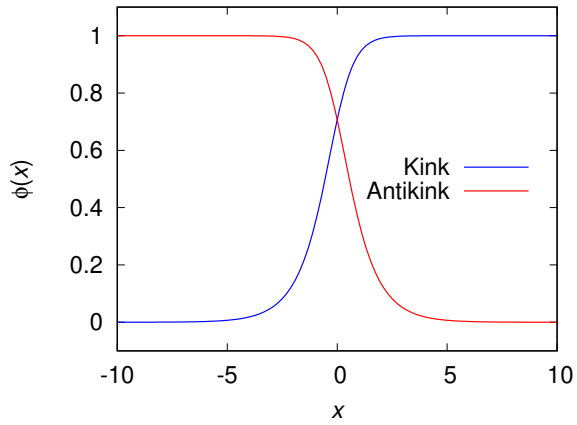

(b) Kink and antikink for topological sector (0,1).

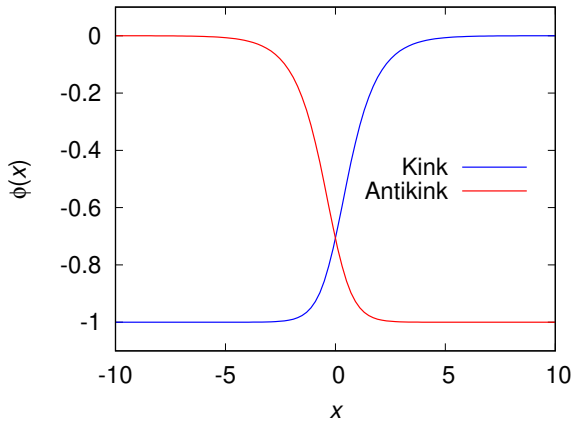

(c) Kink and antikink for topological sector (-1,0).

Figure 1.1: Plots for ϕ^6 model

2. The ϕ^8 field theory

In this chapter we introduce the ϕ^8 model. We will describe this model with the Lagrangian shown in Equation (2.1.1). We would like to understand the model in (1+1) space time dimensions. The potential of the ϕ^8 model is generally given by (Khare et al., 2014)

$$V(\phi) = \lambda^2(\alpha_8\phi^8 - \alpha_6\phi^6 + \alpha_4\phi^4 - \alpha_2\phi^2 + \alpha_0), \tag{2.0.1}$$

where the coefficient of ϕ^8 can be set to $+1$ in the units of λ^2, without loss of generality. So the potential is clearly a polynomial of degree eight. The coefficients of the exponents of ϕ are chosen arbitrarily and one ensures that the minimum of the potential is zero by their choice of α_0 (Khare et al., 2014). The potential will take different shapes, which will depend on our choice of the different coefficients of the polynomial. Gani et al. (2015) studied the ϕ^8 model and used potentials which are non-negative functions of ϕ, the scalar field. We will follow this reference and use potentials with two, three or four degenerate minima. Throughout the essay, we assume that the potentials are symmetric, i.e., $V(-\phi) = V(\phi)$. We will investigate these potentials and the kinks of the model in Chapter 3.

In Section 2.1 we will study (static) solutions and their properties in (1+1) dimensions. In Section 2.2 we introduce kink fluctuations which will be essential in calculating the phase shifts of the ϕ^8 model, which we will discuss in Section 2.3. In Section 2.4 we discuss bound states that arise from solving a scattering problem. Section 2.5 will be dedicated to a discussion of VPEs.

2.1 Kinks in (1+1) dimensions

Let us consider a real scalar field $\phi(t, x)$ of a field-theory in one spatial and one temporal dimension. The Lagrangian density for this system is

$$\mathcal{L} = \frac{1}{2}\partial_\mu\phi\partial^\mu\phi - V(\phi), \tag{2.1.1}$$

where $\mu = 0, 1$. $V(\phi)$ is bounded from below and is a non-negative function of ϕ. First we will consider the action, which is given by

$$\mathcal{S} = \int d^2x\ \mathcal{L}(\phi, \partial_\mu\phi).$$

To find the equations of motion, we first take a functional derivative of this action,

$$\begin{aligned}\delta\mathcal{S}(\phi(t,x)) &= \delta\int_{-\infty}^{\infty} \mathrm{d}^2x\Big[\frac{1}{2}\partial_\mu\phi\partial^\mu\phi - V(\phi)\Big] \\ &= \int_{-\infty}^{\infty} \mathrm{d}^2x\Big[-\partial_\mu\partial^\mu\phi - \frac{dV(\phi)}{d\phi}\Big]\delta\phi.\end{aligned}$$

We obtain the equation of motion for the field by demanding that $\delta\mathcal{S}(\phi(t,x)) = 0$. So, $\delta\mathcal{S}(\phi(t,x)) = 0$ for all $\delta\phi$ if and only if

$$\partial_\mu\partial^\mu(\phi(t,x)) + \frac{\partial V(\phi(t,x))}{\partial\phi} = 0. \tag{2.1.2}$$

For a static configuration, $\phi = \phi(x)$ or $\partial_t \phi = 0$, we have

$$\frac{d^2\phi(x)}{dx^2} = \frac{\partial V(\phi(x))}{\partial \phi},$$

which we integrate with respect to x, to get

$$\frac{d\phi(x)}{dx} = \pm\sqrt{2V(\phi(x))}. \tag{2.1.3}$$

Integrating again with respect to x, we obtain

$$x - x_0 = \pm \int \frac{\mathrm{d}\phi}{\sqrt{2V(\phi(x))}}. \tag{2.1.4}$$

We will take $x_0 = 0$, in the rest of our calculations, except when the degenerate vacua have different curvatures in field space. In this case the VPEs will strongly depend on x_0. We can calculate the classical mass using the integral of the Hamiltonian. So we need to transform this Lagrangian density using

$$\mathcal{H} = \frac{\partial \mathcal{L}}{\partial \dot{\phi}}\dot{\phi} - \mathcal{L},$$

where $\dot{\phi} = \frac{\partial \phi}{\partial t}$ and $\mathcal{H}$ is the Hamiltonian density. In general, the classical Hamiltonian is given by $H = \int \mathcal{H}\mathrm{d}x$, in one spatial dimension. Since for a static configuration we have that $\mathcal{H} = -\mathcal{L}$, then the Hamiltonian density is given by

$$\mathcal{H} = \frac{1}{2}\Big(\partial_x \phi(x)\Big)^2 + V(\phi(x)).$$

Using the energy functional for this Hamiltonian density, we obtain the total energy or mass

$$E[\phi(x)] = \int_{-\infty}^{\infty} \mathcal{H} dx = \int_{-\infty}^{\infty} \left[\frac{1}{2}\Big(\partial_x \phi(x)\Big)^2 + V(\phi(x))\right] \mathrm{d}x. \tag{2.1.5}$$

2.2 Kink Fluctuations

Let us consider a specific soliton, say $\phi_0(x)$. Then we consider a small fluctuation, say $\eta(t, x)$ about this particular soliton,

$$\phi(t, x) = \phi_0(x) + \eta(t, x).$$

If we linearize the field equation, shown in Equation (2.1.2) in $\eta(x, t)$, we obtain

$$\partial_\mu \partial^\mu \eta(t, x) + \left.\frac{\partial^2 V(\phi)}{\partial \phi^2}\right|_{\phi_0(x)} \eta(t, x) = 0.$$

We realize that it takes the form of a Klein-Gordon type equation

$$[\partial_\mu \partial^\mu + U(x)]\eta(t, x) = 0, \tag{2.2.1}$$

where $U(x)$ is the background potential which is generated by the soliton and is given by

$$U(x) = \frac{\partial^2 V(\phi)}{\partial \phi^2}\bigg|_{\phi_0(x)}. \tag{2.2.2}$$

Now we want to know what happens to $U(x)$ at spatial infinity. So, if we let the limit of $U(x)$ take different values as x approaches $-\infty$ and $+\infty$, then

$$\lim_{x\to-\infty} U(x) = m_L^2, \quad \text{and} \quad \lim_{x\to+\infty} U(x) = m_R^2,$$

where m_L^2 and m_R^2 are the squared masses of the quantum fluctuations. This allows us to think about different types of quantum fluctuations. Our next step will be to look at a scattering problem. For such a problem the scattering data include phase shifts and bound states which we will discuss over the next two sections.

2.3 Phase shifts

The sum of scattering phase shifts will be important in the computation of the vacuum polarization energy in Section 2.5 (Weigel, 2017). Consider a stationary wave equation $\eta(x,t) \to e^{-iEt}\eta(x)$, from which we will extract scattering data. We take $m_R \geq m_L$, and we formulate one dimensional scattering, which has been well studied,

$$E^2\eta(x) = [-\partial_x^2 + U(x)]\eta(x) \tag{2.3.1}$$

from Equation (2.2.1). Let us introduce a pseudo-potential which is discontinuous,

$$U_p(x) = U(x) - m_L^2 + (m_L^2 - m_R^2)\Theta(x_m), \tag{2.3.2}$$

where $\Theta(x_m)$ is the step function. Now we have that as $x \to \pm\infty$, $U_p(x) \to 0$. We chose a matching point x_m, which can be any finite point. The stationary equation, Equation (2.3.1), then becomes

$$[-\partial_x^2 + U_p(x)]\eta(x) = \begin{cases} k^2\eta(x), & \text{for} \quad x \leq x_m \\ q^2\eta(x), & \text{for} \quad x \geq x_m \end{cases} \tag{2.3.3}$$

with $k = \sqrt{E^2 - m_L^2}$ and $q = \sqrt{E^2 - m_R^2} = \sqrt{k^2 + m_L^2 - m_R^2}$. Now we solve Equation (2.3.3) and we stress that then we will have solved Equation (2.3.1) as well. Lets us define

$$\begin{aligned} \eta(x) &= A(x)e^{ikx}, \quad \text{for} \quad x \leq x_m, \quad \text{and} \\ \eta(x) &= B(x)e^{iqx}, \quad \text{for} \quad x \geq x_m \end{aligned}$$

with $A(x)$ and $B(x)$ being coefficient functions for the scattering problem. This allows us to write Equation (2.3.3) into the following pair of equations

$$A''(x) = -2ikA'(x) + U_p(x)A(x), \qquad x \leq x_m \tag{2.3.4}$$

$$B''(x) = -2iqB'(x) + U_p(x)B(x), \qquad x \geq x_m \tag{2.3.5}$$

where $A'(x) = \frac{dA(x)}{dx}$ and $B'(x) = \frac{dB(x)}{dx}$. To solve these, we will need boundary conditions, which are $B(\infty) = A(-\infty) = 1$ and $B'(\infty) = A'(-\infty) = 0$. Now matching the solutions at $x = x_m$, we obtain

a scattering matrix S. The diagonal elements of this matrix correspond to the transmission coefficients, and the reflection coefficients are contained on the off-diagonals (Weigel, 2017). We want to find S above and below the threshold. Above the threshold q is real, so we take $k \geq \sqrt{m_R^2 - m_L^2}$, and the scattering matrix becomes

$$S(k) = \begin{pmatrix} e^{-iqx_m} & 0 \\ 0 & e^{ikx_m} \end{pmatrix} \begin{pmatrix} B & -A^* \\ iqB + B' & ikA^* - A'^* \end{pmatrix}^{-1} \begin{pmatrix} A & -B^* \\ ikA + A' & iqB^* - B'^* \end{pmatrix} \begin{pmatrix} e^{ikx_m} & 0 \\ 0 & e^{-iqx_m} \end{pmatrix} \tag{2.3.6}$$

with $A = A(x_m)$ and $B = B(x_m)$. Below the threshold, we will parametrize for $x_m \leq x$, such that $\eta(x) = B(x)e^{-\kappa x}$. Then we replace iq by $\kappa = \sqrt{m_R^2 - m_L^2 - k^2} \geq 0$. Thus, $B(x)$ will be real, and then we will have only the reflection coefficient given by

$$S(k) = -\frac{A(B'/B - \kappa - ik) - A'}{A^*(B'/B - \kappa - ik) - A'^*} e^{2ikx_m}. \tag{2.3.7}$$

Now we calculate the sum of the eigenphase shifts for both the above cases,

$$\delta(k) = -\frac{i}{2}\mathsf{ln}\mathsf{det}S(k) \tag{2.3.8}$$

for $k \in \mathbb{R}$, above and below the threshold. Levinson's theorem (Dong et al., 1998), which relates the phase shifts of the scattered wave at infinite energy and zero energy, states that $\delta(0)$ is usually an odd multiple of $\pi/2$. In Equation (2.3.7), on the right hand side we have a negative sign which agrees with the statement of Levinson's theorem. In our work we consider scattering off a background that does not decompose into channels, then

$$\delta(0) = \pi\Big(n - \frac{1}{2}\Big),$$

where n counts the total number of bound states. Although $\delta(0)$ can in some instances be an integer multiple of π. Examples are reflection-less potentials. Corresponding to $U_p(x) = 0$ is the step potential that is centered at x_m and has a height $m_R^2 - m_L^2$. For $A(x) = B(x) = 1$

$$\delta_{\mathsf{step}}(k) = \begin{cases} (k-q)x_m, & \text{for } k \geq \sqrt{m_R^2 - m_L^2} \\ kx_m - \arctan\Big(\frac{\sqrt{m_R^2 - m_L^2 - k^2}}{k}\Big), & \text{for } k \leq \sqrt{m_R^2 - m_L^2} \end{cases} \tag{2.3.9}$$

agrees with textbook results. It is also essential to find the bound states of Equation (2.3.1). In the next section we look at these so called bound states.

2.4 Bound States

In this section we discuss bound states obtained from solving Equation (2.3.1). Equation (2.3.1) can be solved for three cases (or kinetic regimes). If the energy E is greater than both of the masses of the quantum fluctuations, m_L and m_R, then we only have scattering states (Griffiths, 1994). We can also have a case where the energy is smaller than one of the masses, but greater than the other (for example when the ϕ^8 potential has three degenerate minima which we will see in Section 3.1). Here the solutions propagate to the infinity corresponding to lower mass. So, this is also a scattering state.

Finally, if both of the masses are higher than the energy (E), then we have bound states. In general, these bound states occur when

$$E^2 < m_L^2 \quad \text{and} \quad E^2 < m_R^2.$$

We will solve for the bound states for $E^2 < M_n^2 = 1$ or $k^2 < 0$. We can either have $M_n^2 = m_L^2$ or $M_n^2 = m_R^2$ depending on which of the masses is smaller. So Equation (2.3.1) will become

$$[-\partial_x^2 + U(x)]\eta(x) = (k^2 + M_n^2)\eta(x). \tag{2.4.1}$$

Now we will consider two cases, when $x < x_m$ and $x > x_m$:

i) $x < x_m$

In this case Equation (2.4.1) takes the form

$$[-\partial_x^2 + U_p(x)]\eta(x) = k^2\eta(x), \tag{2.4.2}$$

where $U_p(x) = U(x) - m_L^2$ and $U_p(x) \to 0$ as $x \to -\infty$. We set $k^2 = -\lambda^2$ for $\lambda > 0$. Then $\eta(x) \to A(x)e^{\lambda x}$ as $x \to -\infty$. Therefore, Equation (2.4.2) can be written as

$$\partial_x^2\eta(x) = \lambda^2\eta(x) + U_p(x)\eta(x). \tag{2.4.3}$$

ii) $x > x_m$

In this case Equation (2.4.1) can be written as

$$[-\partial_x^2 + U_p(x) + m_R^2]\eta(x) = k^2\eta(x), \tag{2.4.4}$$

where $U_p(x) \to 0$ as $x \to +\infty$. Again, if we set $k^2 = -\lambda^2$ for $\lambda > 0$, we obtain

$$[-\partial_x^2 + U_p(x)]\eta(x) = -(\lambda^2 + m_R^2)\eta(x). \tag{2.4.5}$$

Let $\kappa = \sqrt{\lambda^2 + m_R^2}$. Then $\eta(x) \to B(x)e^{-\kappa x}$ as $x \to +\infty$. Therefore, Equation (2.4.5) can be written as

$$\partial_x^2\eta(x) = \kappa^2\eta(x) + U_p(x)\eta(x). \tag{2.4.6}$$

Now Equations (2.4.3) and (2.4.6), satisfy the differential equation, shown in Equation (2.4.1) with

$$\eta_R = 1, \quad \eta_R' = -\kappa \text{ as } \quad x \to \infty, \text{ and} \tag{2.4.7}$$
$$\eta_L = 1, \quad \eta_L' = \lambda \text{ as } \quad x \to -\infty. \tag{2.4.8}$$

At x_m we have

$$a\eta_L = b\eta_R \tag{2.4.9}$$
$$a\eta_L' = b\eta_R', \tag{2.4.10}$$

where a and b are linear expansion coefficients. We must find a and b such that the two conditions in Equations (2.4.7) and (2.4.8) hold. So we write Equations (2.4.9) and (2.4.10) in matrix representation

$$\begin{pmatrix} \eta_L & -\eta_R \\ \eta_L' & -\eta_R' \end{pmatrix} \begin{pmatrix} a \\ b \end{pmatrix} = 0. \tag{2.4.11}$$

Equation (2.4.11) can take the form

$$M \begin{pmatrix} a \\ b \end{pmatrix} = 0.$$

If the inverse, M^{-1} of matrix M exists, we will have

$$M^{-1} M \begin{pmatrix} a \\ b \end{pmatrix} = M^{-1} \cdot 0 = 0,$$

implying $(a, b) = (0, 0)$, which is a trivial solution. The trivial solution is not interesting. So we require

$$W = \det \begin{pmatrix} \eta_L & -\eta_R \\ \eta_L' & -\eta_R' \end{pmatrix} = 0,$$

which is known as the Wronskian determinant. Here M^{-1} will not exist. So our task is to make sure that $W = \det M = 0$ is satisfied. Initially, this condition may not be met. So we modify κ in Equation (2.4.6) until we have $W = 0$, then we have a bound state. Generally what we do when we perform the calculation numerically is that we think about a Schrödinger-like equation, where $H = \partial_x^2 + U(x)$. Then our equation will take the form

$$H\eta(x) = \omega^2 \eta(x),$$

where $\omega = 0$ for bound states. We require that $\int dx |\eta(x)|^2 < \infty$, to make sure $\eta(x)$ is normalizable. We have $\eta(x) \to 0$ as $|x| \to \infty$. Starting from negative and positive infinity we integrate the Schrödinger-like equation and try to match them. Initially they do not match, so we adjust κ until they do.

2.5 Vacuum Polarization Energy

The sum of shifts of zero point energies resulting from the interaction with a potential, which in this case is the background potential generated by field ϕ_0 (Weigel, 2017) can be decomposed as

$$E_{\text{vac}}[\phi_0] = \frac{1}{2} \sum_j \left(E_j[\phi_0] - E_j^{(0)} \right) + E_{\text{ct}}[\phi_0]. \tag{2.5.1}$$

Here $E_j[\phi]$ are the eigen energies of the fluctuations in the soliton background. From these we subtract the counterpart without the soliton. Hence this difference is the shift of the zero point energies. The sum of these measures the change of the vacuum (i.e., ground state) energy and is called the renormalizable vacuum polarization energy. The sum in Equation (2.5.1) is a one-loop quantum object and thus ultra-violet divergent. In renormalization theories these divergences are cancelled by counterterms $E_{\text{ct}}[\phi_0]$. The $E_j[\phi_0]$ split into bound and scattering states. We compute the latter contribution by integrating over single particle energies, $\sqrt{k^2 + m_L^2}$, and multiplying by a weight function, $\Delta\rho(k)$, which is the change of the density of states induced by the soliton. We find the density, which is given by $\rho(k) = \frac{dN(k)}{dk}$, for those scattering modes that are incident from negative infinity. This is done by discretizing

$$kL + \delta(k) = N(k)\pi,$$

where the $\delta(k)$ are the phase shifts. Using the condition $L \to \infty$ (continuum limit), and subtracting the result from the non-interacting case, we obtain the Krein formula (Faulkner, 1977)

$$\Delta\rho(k) = \rho(k) - \rho^{(0)}(k) = \frac{1}{\pi} \frac{d}{dk} \delta(k). \tag{2.5.2}$$

For modes incident from positive infinity, the situation is not straight forward. Levels above the threshold are counted by setting

$$qL + \delta(k) = N(k)\pi.$$

There is an additional contribution to the change of density of states, since k is the free states label,

$$\begin{aligned}\frac{L}{\pi}\frac{d}{dk}[q-k] &= \frac{L}{\pi}\frac{d}{dk}\left[\sqrt{k^2+m_L^2-m_R^2}-k\right] \\ &= \frac{L}{\pi}\left[\frac{k}{\sqrt{k^2+m_L^2-m_R^2}}-1\right] \\ &= \frac{L}{\pi}\left[\frac{\sqrt{E^2-m_L^2}}{\sqrt{E^2-m_R^2}}-1\right].\end{aligned}$$

From the Krein formula, we extract the VPE. First integrating by parts and then introducing the no-tadpole renormalization prescription we obtain

$$E_{\text{vac}} = \frac{1}{2}\sum_j (E_j - m_L) - \frac{1}{2\pi}\int_0^\infty \mathrm{d}k \frac{k}{\sqrt{k^2+m_L^2}}\Big(\delta(k) - \delta^{(1)}(k)\Big). \tag{2.5.3}$$

The sum runs over those discrete bound states that exponentially approach zero at spatial infinity. These states are obtained after solving Equation (2.3.1). $\delta^{(1)}(k)$ in Equation (2.5.3) is the Born approximation related to the potential $U(x) - m_L^2$. Unfortunately, we cannot write that

$$\delta^{(1)}(k) \sim \frac{1}{2}\int \mathrm{d}x[U(x) - m_L^2],$$

since for the step potential the Born approximation cannot be written as an integral. Just like Weigel (2017), from Equation (2.3.7) we have that

$$\delta_{\text{step}}(k) \to \frac{x_m}{2k}(m_R^2 - m_L^2) \quad \text{as} \quad k \to \infty.$$

The Born approximation is in fact the first term of the Born series, which can be defined as the expansion of scattering quantities in powers of the interacting potential. Now rewriting Equation (2.3.2) as

$$U(x) - m_L^2 = U_p(x) - (m_L^2 - m_R^2)\Theta(x_m),$$

we can write the Born approximation as

$$\begin{aligned}\delta^{(1)}(k) &= -\frac{1}{2k}\int_{-\infty}^{\infty}\mathrm{d}x U_p(x)\Big|_{x_m} + \frac{x_m}{2k}(m_R^2 - m_L^2) \\ &= -\frac{1}{2k}\int_{-\infty}^{\infty}\mathrm{d}x U_p(x)\Big|_0.\end{aligned}$$

In the end, the Born approximation has no dependence on the matching point x_m, even though $U_p(x)$ was initially defined in terms of x_m. This may just as well be a sign that the VPE is independent of the matching point. The scattering problem will have two channels for a reflection symmetric potential. The channels can either be odd or even. Due to the symmetry we also have $q = k$, and we can continue to $k = it$ analytically for $t \geq 0$. The bound states are collected by integrating over t. The VPE (with this symmetry) is (Graham et al., 2009)

$$E_{\text{vac}}^{(S)} = \int_{m_L}^{\infty} \frac{tdt}{2\pi\sqrt{t^2 - m_L^2}} \left[\ln \left\{ g(t,0) \left(g(t,0) - \frac{1}{t} g'(t,0) \right) \right\} \right]_1 .$$

The subscript indicates that the Born approximation has been subtracted. Here $g(t,x)$ is the Jost solution factor that solves the differential equation

$$g''(t,x) = 2tg'(t,x) + U(x)g(t,x)$$

for imaginary momenta with boundary conditions $g(t,\infty) = 1$ and $g'(t,\infty) = 0$.

3. Numerical results

In this chapter we present the numerical results we obtained. Khare et al. (2014) did an extensive study on phase transitions, and how they occur as a result of the different shapes of the potential. Phase transitions can be defined as the transformations of a system, more specifically a thermodynamic system from one state of matter or phase to another due to heat transfer. This is interesting when studying systems in condensed matter physics. So we will also show different shapes of the potential. First we compute the kinks of the ϕ^8 model for different minima and potential shapes in Section 3.1. We do this by substituting the self-interacting potential into Equation (2.1.4) and evaluating the integral (by partial fractions). The solutions we obtain are implicit. We use nested intervals to come up with numerical solutions and we also present the plots of the kinks. We compute the classical masses as well using Equation (2.1.5).

In Section 3.2 we present phase shifts. In general, we solve a scattering problem (which is a differential equation) to find a scattering matrix. We use this matrix to find the phase shifts and the Born approximation. We also employ adaptive step size in the numerical calculations. Runge Kutta of order four is also used in solving the differential equations.

3.1 Kinks of the ϕ^8 model

In this section we perform a numerical computation of the kink solutions of the ϕ^8 theory. We will use the first integral of the equation of motion, Equation (2.1.4), to find the shapes of the kinks.

3.1.1 Four degenerate minima. In a particular case when the potential has four degenerate minima, at $\phi = \pm a$ and $\phi = \pm b$, then we can factorize the potential as follows

$$V(\phi) = \lambda^2(\phi^2 - a^2)^2(\phi^2 - b^2)^2. \tag{3.1.1}$$

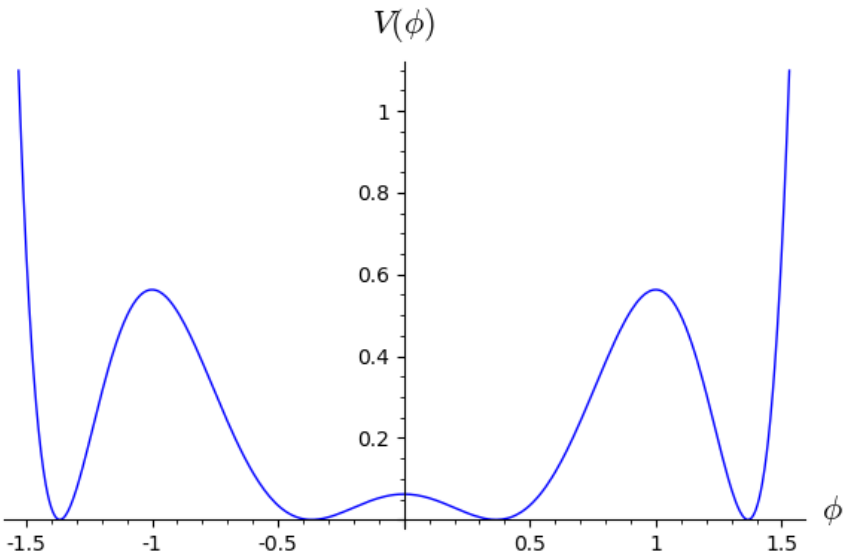

Figure 3.1: Plot of the ϕ^8 potential with four degenerate minima in Equation (3.1.1).

We will use the potential shape, parameterized as in Equation (3.1.1) with $0 < a < b$ and $\lambda > 0$. In fact we will use $b > a$ in this essay. We will use (Khare et al., 2014),

$$a = \frac{-1+\sqrt{3}}{2} \quad \text{and} \quad b = \frac{1+\sqrt{3}}{2}.$$

We show in Figure 3.1 the potential that corresponds to this choice of parameters. We take $\lambda = 1$, but in our calculations we continue with λ and only substitute its value when we do the numerical computations. It can be noted that the curvatures at $\phi = \pm a$ and $\phi = \pm b$ are different, so the kink solutions connecting either a and b or $-b$ and $-a$ will have different mass parameters at negative and positive spatial infinity. For such a potential, Equation (2.1.4) can be written as (with $x_0 = 0$),

$$\sqrt{2}\lambda x = \int \frac{\mathrm{d}\phi}{\sqrt{(\phi^2-a^2)^2(\phi^2-b^2)^2}} = \int \frac{\mathrm{d}\phi}{(\phi^2-a^2)(\phi^2-b^2)}. \tag{3.1.2}$$

There are three topological sectors $(-b,-a)$, $(-a,a)$ and (b,a) to be considered as observed from Figure 3.1. One can deduce that the kink of the topological sector $(-b,-a)$ has similar properties to those of sector (b,a) since the potential is symmetric. So we will only compute the kinks of topological sectors $(-a,a)$ and $(-b,-a)$. The static kink solutions have corresponding antikink solutions. As an example, we will compute the static solutions that interpolate between the vacua $\phi = a$ and $\phi = -a$ at $x \to \infty$ and $x \to -\infty$ respectively. On the other hand, the same vacua are connected by corresponding antikinks interpolating between the vacua $\phi = a$ at $x \to -\infty$ and $\phi = -a$ at $x \to \infty$. Below we compute the kinks from Equation (3.1.2).

Topological sector $(-a,a)$

The kink is bounded by $|\phi| < a$ and $b > a$. So we rewrite Equation (3.1.2) as

$$\sqrt{2}\lambda x = \int \frac{\mathrm{d}\phi}{(a^2-\phi^2)(b^2-\phi^2)}. \tag{3.1.3}$$

We evaluate this integral by partial fractions and obtain

$$2\sqrt{2}\lambda ab(b^2-a^2)x = b\ln\left(\frac{a+\phi}{a-\phi}\right) + a\ln\left(\frac{b-\phi}{b+\phi}\right).$$

Dividing by b and taking the exponential of both sides gives the implicit solution (Lohe, 1979; Gani et al., 2015; Khare et al., 2014)

$$e^{\mu x} = \left(\frac{a+\phi}{a-\phi}\right)\left(\frac{b-\phi}{b+\phi}\right)^{a/b}, \tag{3.1.4}$$

where $\mu = 2\sqrt{2}\lambda a(b^2-a^2)$. The kink is symmetric (Khare et al., 2014). Using Equation (2.1.5), the energy (mass) of this kink was found to be

$$M_{(-a,a)} = \frac{4\sqrt{2}}{15}\lambda a^3(5b^2-a^2), \tag{3.1.5}$$

which we checked numerically. The background potential $U(x)$ is obtained using Equation (2.2.2)

$$U(x) = 56\phi^6 - 60(a^2+b^2)\phi^4 + 12(a^4+4a^2b^2+b^4)\phi^2 - 4a^4b^2 - 4a^2b^4$$

and is shown in Figure 3.2 (b) along with the pseudo-potential. Since $U(a) = U(-a)$, the squared masses of the quantum fluctuations are given by

$$m_R^2 = m_L^2 = 8a^6 - 16a^4b^2 + 8a^2b^4. \tag{3.1.6}$$

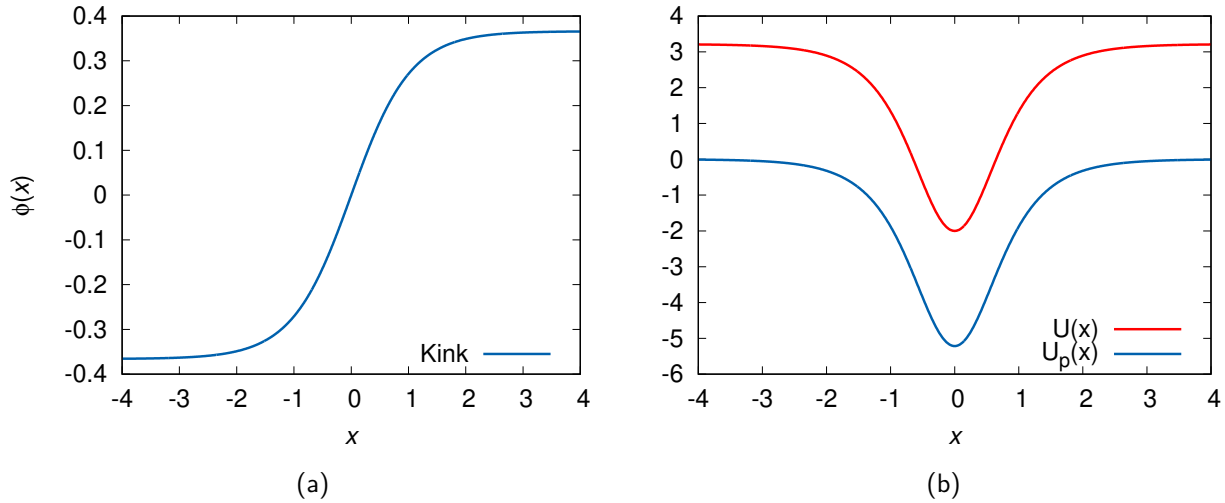

Figure 3.2: (a) Plot of the kink solution of Equation (3.1.4) connecting $-a$ and a. (b) Plot of the background potential $U(x)$ and the pseudo-potential $U_p(x)$.

In Figure 3.2 we show the kink of sector $(-a, a)$ and the background potential $U(x)$. The pseudo potential $U_p(x)$ (shown in Figure 3.2(b)) was also numerically computed from Equation (2.3.2) and we can see that $U_p(x) \to 0$ as $|x| \to \infty$. Using the chosen values of parameters a and b, the classical mass was found to be $M_{(-a,a)} = 0.1701$. From Equation (3.1.6), we found that $m_R^2 = m_L^2 = 3.2154$.

Topological sector $(-b, -a)$

In this sector we have boundary conditions $a < |\phi| < b$, therefore Equation (3.1.2) becomes

$$\sqrt{2}\lambda x = \int \frac{\mathrm{d}\phi}{(\phi^2 - a^2)(b^2 - \phi^2)}, \tag{3.1.7}$$

and by evaluating the integral using partial fractions we obtain

$$2\sqrt{2}\lambda ab(b^2 - a^2)x = b \ln\left(\frac{\phi - a}{\phi + a}\right) + a \ln\left(\frac{b + \phi}{b - \phi}\right),$$

which we simplify to get the implicit solution

$$e^{\mu x} = \left(\frac{\phi - a}{\phi + a}\right)\left(\frac{b + \phi}{b - \phi}\right)^{a/b} \tag{3.1.8}$$

with $\mu = 2\sqrt{2}\lambda a(b^2 - a^2)$. So for the kink connecting $-a$ and $-b$ there is also an exponential behavior to the asymptotes which are now at $\phi = -a, -b$, from

$$\phi(x) = \begin{cases} a + 2a\left(\frac{b-a}{b+a}\right)^{a/b} e^{\mu x}, & x \to -\infty \\ b - 2b\left(\frac{b-a}{b+a}\right)^{a/b} e^{-\mu x b/a}, & x \to +\infty \end{cases}.$$

This implies that the rate at which ϕ asymptotes to $-a$ is μ, and $-\mu b/a$ is the rate at which ϕ asymptotes to $-b$. Therefore, the kink is asymmetric (Khare et al., 2014). Using Equation (2.1.5) again, we obtain the mass of the kink

$$M_{(-b,-a)} = \frac{2\sqrt{2}}{15}\lambda(b-a)^3(a^2+3ab+b^2). \tag{3.1.9}$$

Since the kink connects $-a$ and $-b$, the squared masses of the quantum fluctuations will differ because $U(-b) \neq U(-a)$. The squared masses of the quantum fluctuations are

$$m_R^2 = 8a^6 - 16a^4b^2 + 8a^2b^4, \tag{3.1.10}$$

$$m_L^2 = 8b^6 - 16a^2b^4 + 8a^4b^2. \tag{3.1.11}$$

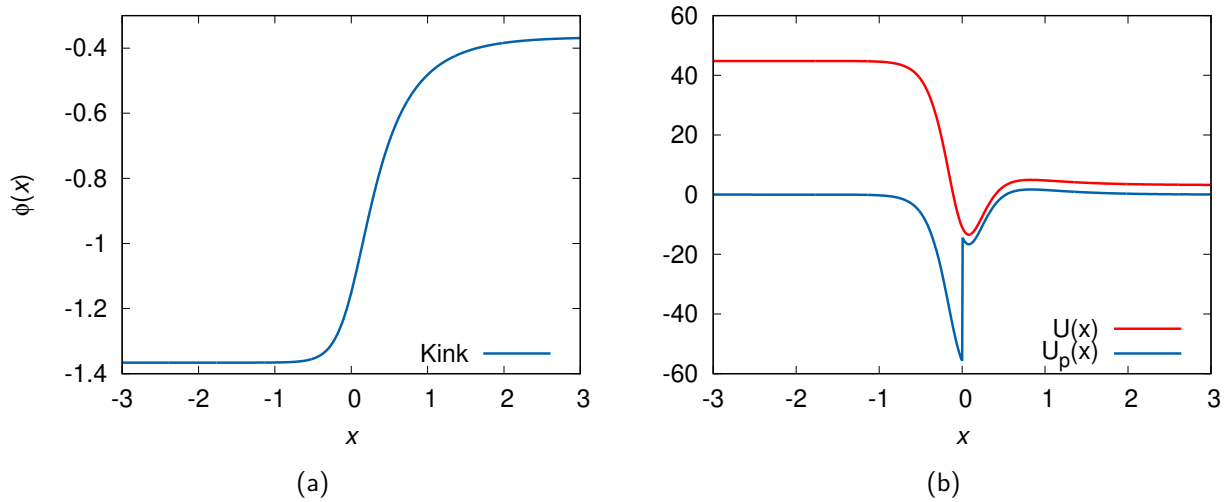

Figure 3.3: (a) Plot of the kink solution of Equation (3.1.8) connecting $-a$ and a. (b) Plot of the background potential $U(x)$ and the pseudo-potential $U_p(x)$.

In Figure 3.3 we have shown the background potential $U(x)$ and the kink of sector $(-b,-a)$. The pseudo potential $U_p(x)$ (shown in Figure 3.3(b)) was also numerically computed from Equation (2.3.2) and we can see that $U_p(x) \to 0$ as $|x| \to \infty$. From Equations (3.1.11) and (3.1.10), we found that $m_L^2 = 44.7846$ and $m_R^2 = 3.2154$ respectively. Using the chosen values of parameters a and b, the classical mass was found to be $M_{(-b,-a)} = 0.65997$ from Equation (3.1.9).

3.1.2 Three degenerate minima. In this situation the potential takes the form

$$V(\phi) = \lambda^2\phi^2(\phi^2-a^2)^2(\phi^2+b^2) \tag{3.1.12}$$

and is shown in Figure 3.4.

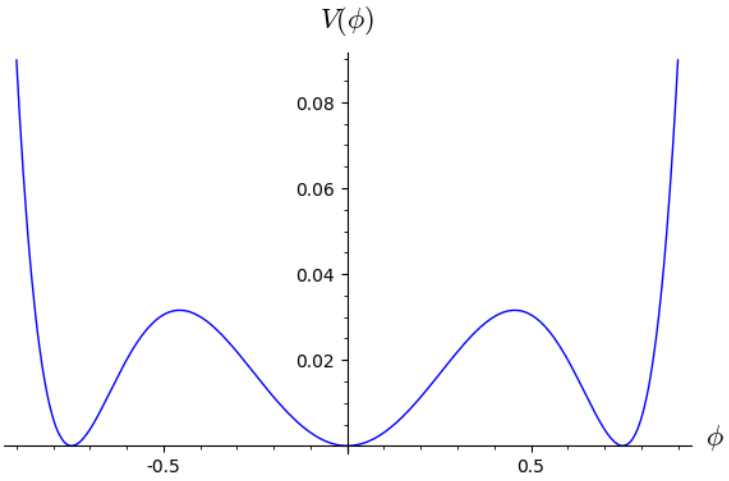

Figure 3.4: Plot of the ϕ^8 potential with three degenerate minima in Equation (3.1.12).

The constants in Equation (3.1.12) satisfy $a > 0$, $b > 0$, and $\lambda > 0$. The three minima of the potential are: $\bar{\phi}_1 = -a$, $\bar{\phi}_2 = 0$ and $\bar{\phi}_3 = a$. So the topological sectors will be $(-a, 0)$ and $(0, a)$. We choose the parameters, (Khare et al., 2014)

$$a = \frac{3}{4}, \quad b = 1. \tag{3.1.13}$$

We will study one of $(-a, 0)$ and $(0, a)$, because they are obviously related by a change of sign of $\phi(t, x)$. Here Equation (3.1.2), together with the potential gives

$$\sqrt{2}\lambda x = \int \frac{\mathrm{d}\phi}{\phi(\phi^2 - a^2)\sqrt{\phi^2 + b^2}}. \tag{3.1.14}$$

We evaluate the integral, making use of partial fractions and obtain,

$$2\sqrt{2}\lambda a^2\sqrt{a^2 + b^2}x = \ln\left(\frac{\sqrt{b^2 + a^2} + \sqrt{b^2 + \phi^2}}{\sqrt{b^2 + a^2} - \sqrt{b^2 + \phi^2}}\right) + \frac{\sqrt{b^2 + a^2}}{b}\ln\left(\frac{\sqrt{b^2 + \phi^2} - b}{\sqrt{b^2 + \phi^2} + b}\right),$$

which simplifies to the implicit solution,

$$e^{\mu x} = \left(\frac{\sqrt{b^2 + a^2} + \sqrt{b^2 + \phi^2}}{\sqrt{b^2 + a^2} - \sqrt{b^2 + \phi^2}}\right)\left(\frac{\sqrt{b^2 + \phi^2} - b}{\sqrt{b^2 + \phi^2} + b}\right)^{\sqrt{b^2+a^2}/b} \tag{3.1.15}$$

with $\mu = 2\sqrt{2}\lambda a^2\sqrt{b^2 + a^2}$. The mass of the kink was found, using Equation (2.1.5), to be

$$M_{(0,a)} = \frac{\sqrt{2}}{15}\lambda(2(b^2 + a^2)^{5/2} - b^3(2b^2 + 5a^2)). \tag{3.1.16}$$

Here, the background potential is

$$U(x) = 56\phi^6 - 30(2a^2 - b^2)\phi^4 + 12(a^4 - 2a^2b^2)\phi^2 + 2a^4b^2$$

and is shown in Figure 3.5. The squared masses of the quantum fluctuations are given by

$$m_R^2 = 8a^6 + 8a^4b^2, \tag{3.1.17}$$

$$m_L^2 = 2a^4b^2, \tag{3.1.18}$$

and we see that they differ since $U(0) \neq U(a)$.

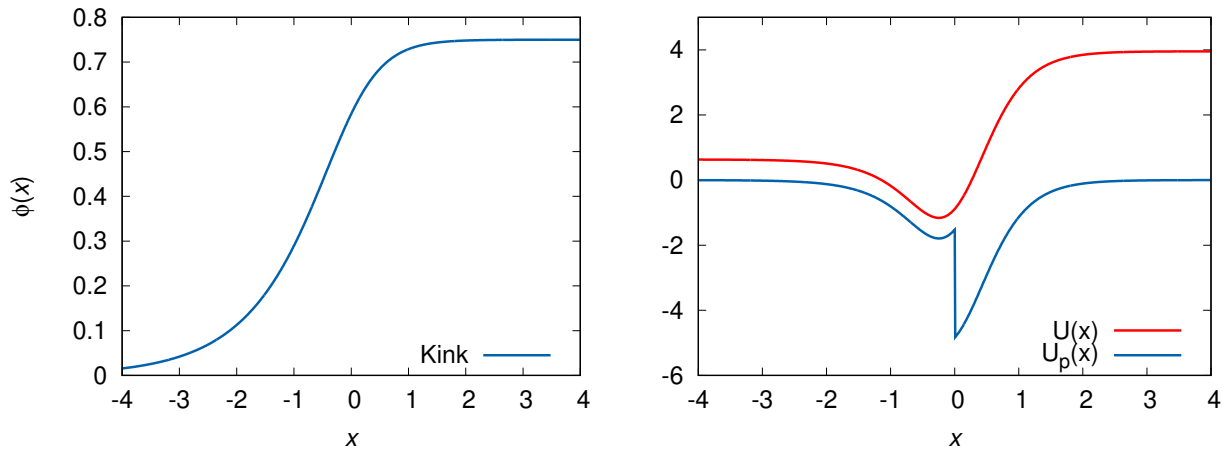

(a) (b)

Figure 3.5: (a) Plot of the kink solution of Equation (3.1.4) connecting $-a$ and a. (b) A plot of the background potential $U(x)$ and the pseudo-potential $U_p(x)$.

Figure 3.5 shows the kink of sector $(-a, a)$ and the background potential $U(x)$. The pseudo potential $U_p(x)$ (shown in Figure 3.5(b)) was also numerically computed from Equation (2.3.2) and we can see that $U_p(x) \to 0$ as $|x| \to \infty$. Using the chosen values of parameters a and b, the classical mass was found to be $M_{(0,a)} = 0.1217$. The squared masses of the fluctuations were found to be $m_L^2 = 0.6328$ and $m_R^2 = 3.9551$ using Equations (3.1.18) and (3.1.17), respectively.

3.1.3 Two degenerate minima. The potential of the ϕ^8 model with two minima takes the form

$$V(\phi) = \lambda^2(\phi^2 - a^2)^2(\phi^2 + b^2)^2, \tag{3.1.19}$$

with minima $\phi = \pm a$. The potential is shown in Figure 3.6.

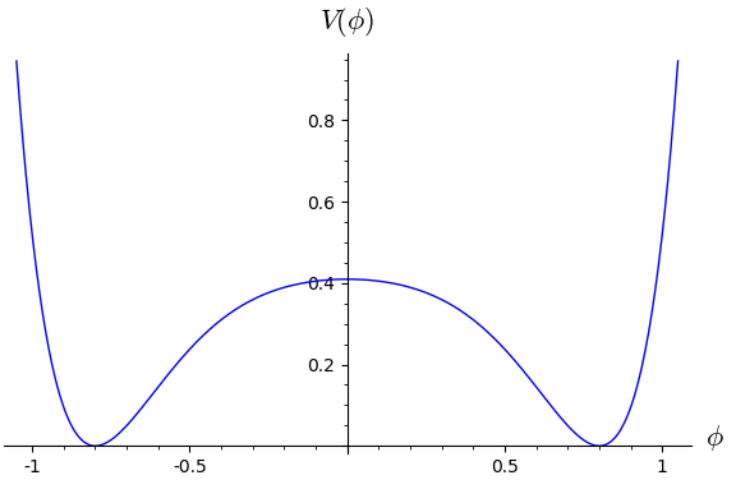

Figure 3.6: Plot of the ϕ^8 potential with three degenerate minima in Equation (3.1.19).

Here $a > 0$, $b > 0$, and $\lambda > 0$. Again, we will use parameters (Khare et al., 2014)

$$a = \frac{4}{5} \quad b = 1.$$

Then Equation (3.1.2), with the potential of Equation (3.1.19) gives

$$\sqrt{2}\lambda x = \int \frac{\mathrm{d}x}{(\phi^2 - a^2)(\phi^2 + b^2)}, \tag{3.1.20}$$

which we integrate to get

$$2\sqrt{2}\lambda a(b^2 + a^2)x = \frac{2a}{b}\arctan\left(\frac{\phi}{b}\right) + \ln\left(\frac{\phi + a}{\phi - a}\right).$$

Setting $\mu = 2\sqrt{2}\lambda a(b^2 + a^2)$ allows us to write

$$\mu x = \frac{2a}{b}\arctan\left(\frac{\phi}{b}\right) + \ln\left(\frac{\phi + a}{\phi - a}\right), \tag{3.1.21}$$

which is again an implicit solution. The mass of the kink is (using Equation (2.1.5))

$$M_{(-a,a)} = \frac{4\sqrt{2}}{15}\lambda a^3(a^2 + 5b^2). \tag{3.1.22}$$

The background potential $U(x)$ is

$$U(x) = 56\phi^6 - 60(a^2 - b^2)\phi^4 + 12(a^4 - 4a^2b^2 + b^4)\phi^2 + 4a^4b^2 - 4a^2b^4,$$

and we have plotted it in Figure 3.7. Now since $U(a) = U(-a)$, the squared masses of the quantum fluctuations are given by

$$m_R^2 = m_L^2 = 8a^6 + 16a^4b^2 + 8a^2b^4.$$

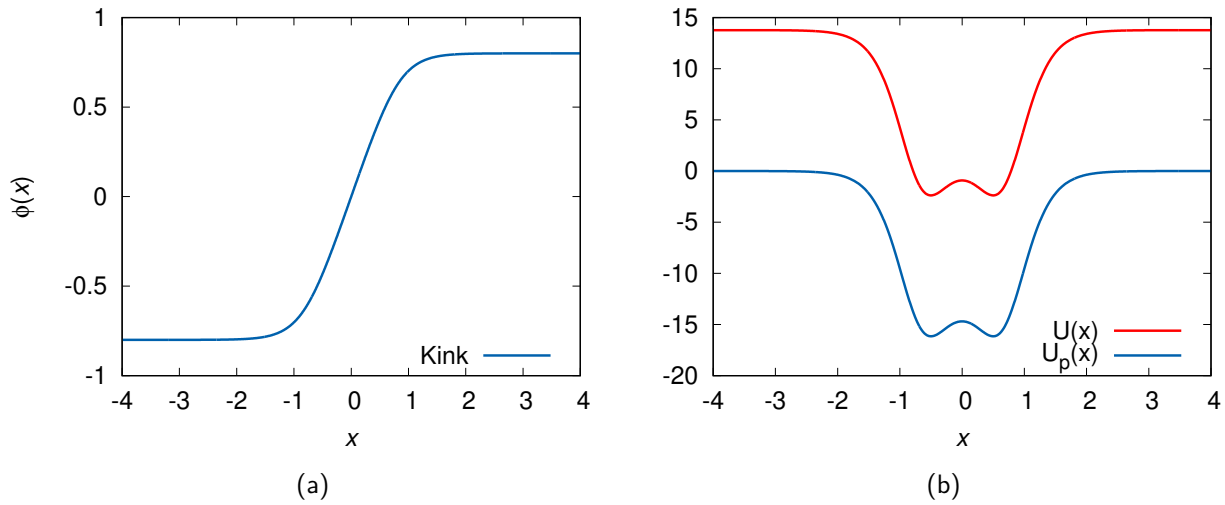

(a) (b)

Figure 3.7: (a) Plot of the kink solution of Equation (3.1.21) connecting $-a$ and a. (b) Plot of the background potential $U(x)$ and the pseudo-potential $U_p(x)$.

In Figure 3.7 we show the kink that connects vacua a and $-a$ and the background potential $U(x)$. We computed numerically the pseudo potential $U_p(x)$ (shown in Figure 3.7(b)) from Equation (2.3.2) and we can see that $U_p(x) \to 0$ as $|x| \to \infty$. Using the chosen values of parameters a and b, the classical mass was found to be $M_{(-a,a)} = 1.0890$. From Equation (3.1.6), we found that $m_R^2 = m_L^2 = 13.7708$.

The next step is to put into the scattering problem the potential of each kink. Then we proceed to computing the scattering matrix. From this matrix we will do a numerical computation of the phase shifts and the Born approximation in the section that comes next. There are a number of reasons that make the scattering matrix important. We can use it to compute the sum of the eigenphase shifts, which we did in this work. The scattering matrix must be unitary, to properly relate the initial and final states of the scattering. In quantum mechanics this unitary property is related to the conservation of what is known as the probability current. However there is an issue here. Equation (2.3.5) does not give a unitary S-matrix when $m_L \neq m_R$. In this case additional flux factors must be added. However they leave Equation (2.3.8) invariant.

3.2 Phase Shifts and Born approximation

In this section we will present the sum of the eigenphase shifts $\delta(k)$ obtained from the scattering matrix. First we choose five momentum values and write out what the phase shifts are for three different matching points. These are shown in Table 3.1 for the topological sector $(-a, a)$. What we see when we change the matching point is that the sum of the eigenphase shifts remains the same. This tells us that the scattering matrix, $S(k)$, is independent of the matching point, since $\delta(k)$ is calculated from $S(k)$. This is a litmus test of our numerical simulation, as the matching point is an artificial concept.

k	1.000	3.825	7.550	11.275	15.000
$x_m = -1$					
$\delta(k)$	1.57641	1.19767	0.630585	0.425611	0.320830
$x_m = 0$					
$\delta(k)$	1.57639	1.19767	0.630584	0.425611	0.320830
$x_m = 3$					
$\delta(k)$	1.57641	1.19767	0.630585	0.425611	0.320830

Table 3.1: Numerical phase shifts $\delta(k)$ for chosen momentum k.

In Figure 3.8 we show the sum of the eigenphase shifts. Doing a numerical calculation of Equation (2.3.8) leads to a discontinuous function in $[-\pi/2, \pi/2]$. We carefully add multiples of π to do away with these discontinuities. We must have that as $k \to \infty$, $\delta(k)$ goes to zero. This can be seen in Figure 3.8 and it so happens that it aligns with the Born approximation as $k \to \infty$. We can recall from Equation (3.1.6) that $m_R^2 = m_L^2$, therefore the phase shift in Figure 3.8 is a continuous function of the momentum. At $k = 0$ we computed $\delta(k)$ numerically and we find $\delta(0) = 1.5\pi$ with two bound states.

The bound states we obtained from solving Equation (2.3.1) are presented here. The number of bound states (n) is obtained from the sum of eigenphase shifts and is given by

$$n = \frac{1}{\pi}\delta(k)\Big|_{k=0} + \frac{1}{2}. \tag{3.2.1}$$

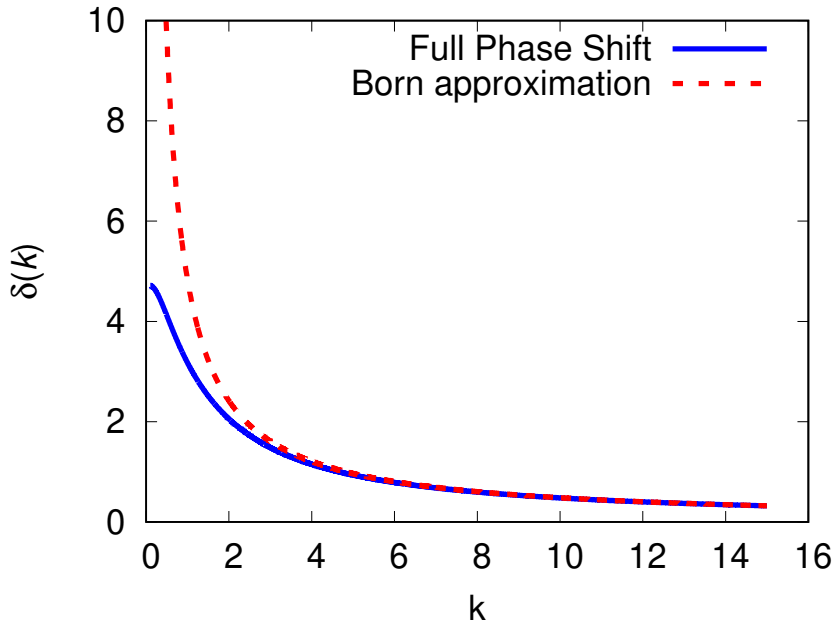

Figure 3.8: Full phase shift and Born approximation of the topological sector $(-a, a)$.

For the topological sector $(-a, a)$ we have

$$n = \frac{1}{\pi} \cdot 1.5\pi + \frac{1}{2} = 2. \tag{3.2.2}$$

We show this in Table 3.2, which shows the eigenvalues of the kinks in Equations (3.1.4), (3.1.8), (3.1.15) and (3.1.21). These were computed by Gani et al. (2014). We have only computed the bound states for the kink Equation (3.1.4). The other three kinks were also computed in Gani et al. (2014) and we intend to compute them as well.

We have been able to compute numerically the phase shifts for the topological sector $(-a, a)$ in this work. It takes four days to a week on a computer cluster to come up with this data. We were not able to compute the data for the rest of the kink solutions in time (but we are still working towards this). This data includes the VPE and the bound states for the other kinks. Currently, we are trying to compute the phase shifts for other kinks and their bound states. These will be essential in the computation of VPE. For example, the kink connecting vacua $-b$ and $-a$ in the particular case when the potential has four degenerate minima, connects vacua with different curvatures for the fluctuations. This may potentially lead to unbounded VPE that destabilizes the soliton.

Kink	x_{min}	x_{max}	E_j^2	$\delta(0)$	n
Equation (3.1.4)	-9	9	$E_0^2 = -2 \times 10^{-8}$ $E_1^2 = 2.70491$	1.5π	2
Equation (3.1.8)	-9	9	$E_0^2 = -7 \times 10^{-8}$	$\frac{\pi}{2}$	1
Equation (3.1.15)	-42	13	$E_0^2 = 4 \times 10^{-8}$	$\frac{\pi}{2}$	1
Equation (3.1.21)	-10	10	$E_0^2 = 5 \times 10^{-9}$ $E_1^2 = 4.27575$ $E_2^2 = 10.1893$ $E_1^2 = 13.6095$	3.5π	4

Table 3.2: Bound States.

4. Conclusion

We have computed the kink solutions of the ϕ^8 field model for three different parameters of the model in one temporal and one spatial dimension. We studied quantum fluctuations about specific static solitons. This allowed us to formulate a scattering problem. To study this problem we computed a scattering matrix $S(k)$. We also computed a sum, $\delta(k)$, of eigenphase shifts and Born approximation from $S(k)$. We obtained that as $k \to \infty$, $\delta(k)$ and the Born approximation agree as they both go to zero. We also found that bound states can be calculated from $\delta(k)$ at $k = 0$. We also computed the classical energies and discussed techniques to compute quantum correction (VPE) to these classical energies. These techniques make handy use of the phase shifts. Here we have presented for the first time computation of phase shifts for the fluctuations around a kink in the ϕ^8 model.

4.1 Future work

The numerics for small values of k will be checked and compared against the theory. It will be relevant to compute the bound states. The VPE will also be computed from these data. It will be interesting to see their contributions to the various sectors. It will also be interesting to see how the VPE depend on x_0 in the sectors where $m_L \neq m_R$. The VPE should not depend on x_0 if $m_L = m_R$.

Acknowledgements

First and foremost, I will like to thank God for always being the provider. My gratitude goes to my supervisor Prof. Herbert Weigel for guiding me as I carried out this work. He has introduced me to the fascinating field of field theories. He has worked tirelessly to make sure I carried out this work with understanding, even though I did not have much background in Quantum Field theory and was patient with me. I would also like to thank my parents, who have been my main source of support, even though I am far from home. They have encouraged me even before I came to AIMS. I would like to extend my gratitude to the AIMS family, Jeff, Barry, Jan and Mastercard Foundation funding my study at AIMS. I would like extend my gratitude to my Tutor Lila, for helping me with my essay. Many thanks to my friends, who made my AIMS experience one that I will never forget.

References

Belendryasova, E. and Gani, V. A. Scattering of the φ^8 kinks with power-law asymptotics. *Communications in Nonlinear Science and Numerical Simulation*, 67:414–426, 2019.

Dong, S.-H., Hou, X.-W., and Ma, Z.-Q. Relativistic levinson theorem in two dimensions. *Physical Review A*, 58(3):2160, 1998.

Drazin, P. G. and Johnson, R. S. *Solitons: an introduction*, volume 2. Cambridge University Press, 1989.

Faulkner, J. Scattering theory and cluster calculations. *Journal of Physics C: Solid State Physics*, 10 (23):4661, 1977.

Gani, V. A., Kudryavtsev, A. E., and Lizunova, M. A. Kink interactions in the (1 + 1)-dimensional φ^6 model. *Physical Review D*, 89(12):125009, 2014.

Gani, V. A., Lensky, V., and Lizunova, M. A. Kink excitation spectra in the (1 + 1)-dimensional φ^8 model. *Journal of High Energy Physics*, 2015(8):147, 2015.

Graham, N., Quandt, M., and Weigel, H. *Spectral methods in quantum field theory*, volume 777. Springer, 2009.

Griffiths, D. J. *Introduction to quantum mechanics*. Pearson international edition (Pearson Prentice Hall, 1995), 1994.

Khare, A., Christov, I. C., and Saxena, A. Successive phase transitions and kink solutions in ϕ^8, ϕ^{10}, and ϕ^{12} field theories. *Physical Review E*, 90(2):023208, 2014.

Korteweg, D. J. and De Vries, G. Xli. On the change of form of long waves advancing in a rectangular canal, and on a new type of long stationary waves. *The London, Edinburgh, and Dublin Philosophical Magazine and Journal of Science*, 39(240):422–443, 1895.

Kosevich, A., Gann, V., Zhukov, A., and Voronov, V. Magnetic soliton motion in a nonuniform magnetic field. *Journal of Experimental and Theoretical Physics*, 87(2):401–407, 1998.

Lohe, M. Soliton structures in P($\varphi)_2$. *Physical Review D*, 20(12):3120, 1979.

MacPherson, D. C. *Quantum fluctuations and soliton generation in stimulated Raman scattering*. PhD thesis, Montana State University-Bozeman, College of Letters & Science, 1989.

Manton, N. and Sutcliffe, P. *Topological solitons*. Cambridge University Press, 2004.

Marjaneh, A. M., Gani, V. A., Saadatmand, D., Dmitriev, S. V., and Javidan, K. Multi-kink collisions in the ϕ^6 model. *Journal of High Energy Physics*, 2017(7):28, 2017.

Saxena, A., Christov, I. C., and Khare, A. Higher-order field theories: ϕ^6, ϕ^8 and beyond. In *A Dynamical Perspective on the ϕ^4 Model*, pages 253–279. Springer, 2019.

Scott, A. Davydov's soliton. *Physics Reports*, 217(1):1–67, 1992.

Skyrme, T. A non-linear field theory. *Proceedings of the Royal Society of London. Series A. Mathematical and Physical Sciences*, 260(1300):127–138, 1961.

Vilenkin, A. and Shellard, E. P. S. *Cosmic strings and other topological defects*. Cambridge University Press, 2000.

Weigel, H. Vacuum polarization energy for general backgrounds in one space dimension. *Physics Letters B*, 766:65–70, 2017.

Weigel, H. and Graham, N. Vacuum polarization energy of the shifman–voloshin soliton. *Physics Letters B*, 783:434–439, 2018.

Yousefi, Y. and Muminov, K. K. A simple classification of solitons. *arXiv preprint arXiv:1206.1294*, 2012.

Zabusky, N. J. and Kruskal, M. D. Interaction of "solitons" in a collisionless plasma and the recurrence of initial states. *Physical review letters*, 15(6):240, 1965.